MITSUBISHI ELECTRIC RESEARCH LABORATORIES
http://www.merl.com

A Reconfigurable Plug-and-Play Model Predictive Controller for Multi-Evaporator Vapor Compression Systems

Zhou, J.; Burns, D.J.; Danielson, C.; Di Cairano, S.

TR2016-048 July 2016

Abstract

This paper presents a reconfigurable Plug-andPlay (PnP) Model Predictive Controller (MPC) for multievaporator vapor compression systems (VCS) where individual evaporators are permitted to turn on or off. This alters the number of performance variables, actuators and constraints. The proposed approach features structural online updates of the closed loop system with stability guarantees, and avoids the need to commission and tune separate controllers for when individual subsystems are turned on or off. To compare the performance of the proposed approach, a more conventional switched MPC is also developed in order to provide a benchmark design, wherein separate model representations are developed and controllers with numerous tuning parameters are synthesized and deployed depending on the VCS operation mode. Simulations are provided comparing the performance of the proposed reconfigurable PnP MPC to the traditionally-designed switched MPC. Results confirm that the reconfigurable PnP MPC maintains the same performance as the switched MPC approach in terms of room temperature reference tracking after zones are switched on, enforcement of critical machine constraints, and disturbance rejection. However, reconfigurable PnP MPC requires no extra tuning or controller design effort, and can be automatically synthesized from a single master controller design for any VCS operating mode.

2016 American Control Conference (ACC)

A Reconfigurable Plug-and-Play Model Predictive Controller for Multi-Evaporator Vapor Compression Systems

Junqiang Zhou, Daniel J. Burns,† Claus Danielson, and Stefano Di Cairano

***Abstract*— This paper presents a reconfigurable Plug-and-Play (PnP) Model Predictive Controller (MPC) for multi-evaporator vapor compression systems (VCS) where individual evaporators are permitted to turn on or off. This alters the number of performance variables, actuators and constraints. The proposed approach features structural online updates of the closed loop system with stability guarantees, and avoids the need to commission and tune separate controllers for when individual subsystems are turned on or off. To compare the performance of the proposed approach, a more conventional switched MPC is also developed in order to provide a benchmark design, wherein separate model representations are developed and controllers with numerous tuning parameters are synthesized and deployed depending on the VCS operation mode.**

Simulations are provided comparing the performance of the proposed reconfigurable PnP MPC to the traditionally-designed switched MPC. Results confirm that the reconfigurable PnP MPC maintains the same performance as the switched MPC approach in terms of room temperature reference tracking after zones are switched on, enforcement of critical machine constraints, and disturbance rejection. However, reconfigurable PnP MPC requires no extra tuning or controller design effort, and can be automatically synthesized from a single master controller design for any VCS operating mode.

I. INTRODUCTION

Vapor compression systems (VCS), such as heat pumps, refrigeration and air-conditioning systems, are widely used in industrial and residential applications. The introduction of variable speed compressors, electronically-positioned valves, and variable speed fans to the vapor compression cycle has greatly improved the flexibility of the operation of such systems (Fig. 1). This increased actuator flexibility, along with increasing onboard computational power, enables more sophisticated control schemes than traditional on-off logic, or decoupled PI controllers. For example, Model Predictive Control (MPC) of vapor compression systems offers a flexible and rigorous design process in which the constraints are enforced during transients and can be modified as the design evolves. Furthermore, by appropriate designs, the resulting controller provides guarantees on feasibility, optimality, convergence, transient performance and stability [1], [2].

Prior work on predictive control of multi-evaporator systems have exploited the repeated evaporators and associated mechanical elements to identify symmetries in the underlying model structure [3], and in fact, similar observations underpin the current work. This structure has lead several groups to propose decentralized controller architectures [4], [5], motivated primarily by an effort to overcome computational challenges associated with centralized approaches. However, prior approaches consider only fixed-operation machines where the number of active evaporators does not change. In practice, however, many multi-evaporator systems often experience low heat loads in localized zones such that a particular evaporator no longer needs to provide cooling and should be shut off while the remaining evaporators continue to provide service. Despite the promising advantages of model predictive control on vapor compression systems, key challenges remain to extend the approach to a multi-evaporator system where individual evaporators can be turned on or off independently, e.g., by closing the valves that allow refrigerant to enter the evaporator and shutting off the associated fan. Turning subsystems on or off alters the structure of the prediction model and changes the number of regulated variables, actuators, sensors, and constraints. A structural change of this nature typically requires a separate controller for each machine operating mode (also known as monolithic control design) [6], [7].

However, recent work has extended Youla-Kucera parameterization to controller structural modification which has resulted in the flexibility to add or remove the number of actuators and sensors from the controller during online operation and has been termed ‘plug-and-play’ (PnP) control [7]. The PnP model predictive control has also been developed for complex networks based on decentralized [8] and distributed [9] approaches motivated by the time-varying network topology in which subsystems join or leave the network. These proposed approaches require a re-design of the controllers to guarantee stability in response to changing network conditions.

Considering that the control re-design for MPC typically requires either complex online computations or deployment of large pre-designed controller parameters into the hardware, it is difficult to practically implement such algorithms on vapor compressor machines with microprocessors having limited computational capabilities and memory. Therefore, this paper proposes a *reconfigurable* plug-and-play MPC design by exploiting the repeated subsystem model structure that emerges from multiple connected evaporators in parallel to a compressor and condenser. The proposed approach features a single control law designed for the situation when all subsystems are turned on, and enables automatic synthesis of controllers for operating modes when any number of

J. Zhou is with Center for Automotive Research, The Ohio State University, 930 Kinnear Rd., Columbus, OH, 43212, USA. Email: zhou.412@osu.edu

D. J. Burns, C. Danielson and S. Di Cairano are with Mitsubishi Electric Research Laboratories, Cambridge, MA, Email: burns@merl.com, danielson@merl.com, dicairano@merl.com

† Corresponding author.

evaporators are turned off. In this way, a single controller can be designed and tuned based on a single appropriately-partitioned prediction model, and can scale to any combination of active evaporators in a multi-evaporator VCS. Further, the reconfigurable MPC design is compared with a switched MPC design both in terms of closed loop system performance and practical implications of controller reconfiguration such as the engineering effort required to synthesize, tune and validate a controller for each instance of system operation.

The paper is organized as follows: Section II gives a description of the model and associated augmentations. The reconfigurable MPC design is proposed in Section III. Finally, simulation and comparison results against a switched MPC design are presented in Section IV with concluding remarks offered in Section V.

Notation: For $x \in \mathbb{R}^n, y \in \mathbb{R}^m$, we define $\text{col}(x, y) := [x^T \quad y^T]^T$ and $\|x\|_P^2 := x^T P x$. Denote $\mathbb{Z} := \{0, 1, ...\}$ as the set of nonnegative integer numbers. The direct-sum of matrices $G_1 \in \mathbb{R}^{n_1 \times m_1}$ and $G_2 \in \mathbb{R}^{n_2 \times m_2}$ is denoted as $G_1 \oplus G_2 := \left[\begin{smallmatrix} G_1 & 0 \\ 0 & G_2 \end{smallmatrix}\right] \in \mathbb{R}^{(n_1+n_2)\times(m_1+m_2)}$. Let $\mathcal{X}$ be a convex polyhedral set of the form $\mathcal{X} := \{x : F_i x \le g_i, \quad i = 1, 2, ...\}$. Then, a soft constrained set $\mathcal{X}_\epsilon$ with a slack variable ϵ is expressed as $\mathcal{X}_\epsilon := \{x : F_i x \le g_i + \epsilon, \quad i = 1, 2, ...\}$.

Elementary matrix operation to zero out non-zero entries in i-th row and j-th column of a matrix $P \in \mathbb{R}^{n\times m}$ can be obtained by pre- and post- multiplying matrices as $\Theta_i P$ and $P\Theta_j$, where $\Theta_i \in \mathbb{R}^{n\times n}$ and $\Theta_j \in \mathbb{R}^{m\times m}$ are diagonal matrices with unitary entries except i-th and j-th entry being zero, respectively.

II. Control Model Description

A. Multi-Evaporator System Model Description

This study considers a multi-evaporator vapor compression system with N indoor units as shown in Fig. 1. In particular, we use subscript 0 to represent the refrigerant system (e.g., the compressor, outdoor unit heat exchanger and associated fan), which will be referred as “centralized system” and can be described with an LTI model:

$$x_{e_0}(t+1) = A_{e_{00}} x_{e0}(t) + \sum_{i=0}^{N} B_{e_{0i}} u_{e_i}(t),$$
$$z_{e_0}(t) = E_{e_0} x_{e_0}(t), \qquad y_{e_0}(t) = C_{e_0} x_{e_0}(t). \qquad (1)$$

Moreover, we use subscript $i \in \{1, ..., N\}$ to represent i-th zone temperature dynamics (principally the dynamics associated with each evaporator and associated zone air), which will be referred as “decentralized system” and can be written as set of LTI models:

$$x_{e_i}(t+1) = A_{e_{ii}} x_{e_i}(t) + A_{e_{i0}} x_{e_0}(t) + \sum_{j=0}^{N} B_{e_{ij}} u_{e_i}(t),$$
$$z_{e_i}(t) = E_{e_i} x_{e_i}(t), \quad \forall i = 1, ..., N, \qquad (2)$$

where $x_{e_i}, u_{e_i}, z_{e_i}$, for $i \in \{0, 1, ..., N\}$ represent states, control inputs and performance outputs, respectively and y_{e_0} represents constrained outputs of the centralized system, as shown in Table I. To simplify the notation, we denote $\mathcal{N} := \{1, ..., N\}$ as the index of decentralized-only subsystems and $\mathcal{N}_0 := \{0, 1, ..., N\}$ with respect to the entire subsystems.

TABLE I

Definition of Physical Signals

Signal Type	Signal Symbol	Signal Description	Units
Control Inputs	u_{e_0}	compressor frequency (CF)	Hz
		outdoor (condenser) fan speed (ODF)	rpm
	u_{e_i}	cooling capacity of i-th zone (CCC)	%
Performance Outputs	z_{e_0}	discharge temperature (Td)	^{o}C
	z_{e_i}	i-th zone temperature (Tri)	^{o}C
Constrained Outputs	y_{e_0}	discharge temperature (Td)	^{o}C
		evaporating temperature (Te)	^{o}C
		condensing temperature (Tc)	^{o}C
References	r_0	discharge temperature (Td ref)	^{o}C
	r_i	i-th zone temperature (Tri ref)	^{o}C

Note that the performance outputs $z_{e_0} \in \mathscr{Z}_{e_0}$ are a subset of the constrained outputs $y_{e_0} \in \mathscr{Y}_{e_0}$, that is, $\mathscr{Z}_{e_0} \subset \mathscr{Y}_{e_0}$. The constrained outputs only consist of variables associated with the centralized systems, and the outputs for each zone relate only to temperature regulation, thus they are not enforced with constraints. The output $y_{e_0}(t) \in \mathcal{Y}$ and input $u_{e_i}(t) \in \mathcal{U}_i, \ \forall i = \mathcal{N}_0$ constraint sets are compact, convex and containing the origin in their interior.

B. Prediction Model Development

The MPC relies on linear models to predict the system output response and to determine the optimal control inputs that achieve the tracking of performance output and guarantee that the constrained outputs remain within their bounds. However, predicted outputs can deviate from measured values in the presence of disturbances and modeling errors. To account for such errors, the output equations are augmented with offset terms

$$y_{e_0}(t) = C_{e_0} x_{e_0}(t) + w_{e_0}(t),$$
$$z_{e_i}(t) = E_{e_i} x_{e_i}(t) + w_{e_i}(t), \qquad \forall i \in \mathcal{N}, \qquad (3)$$

where $w_{e_i}, i \in \mathcal{N}_0$ denote the auxiliary offset states [10] that are constant over the prediction horizon, $w_{e_i}(t+1) = w_{e_i}(t)$. Since $\mathscr{Z}_{e_0} \subset \mathscr{Y}_{e_0}$, there exists a natural projection $H_{e_0} : \mathscr{Y}_{e_0} \to \mathscr{Z}_{e_0}$ such that $z_{e_0}(t) = E_{e_0} x_{e_0}(t) + H_{e_0} w_{e_0}(t)$.

Remark 1: Following a standard procedure [10], a Kalman filter observer [1] can be designed based on state equations in (1)-(2) and output equation in (3) to estimate the state value $x_{e_i}(t), i \in \mathcal{N}_0$ and output offset value $w_{e_i}(t), i \in \mathcal{N}_0$ at each sampling time. The estimated information is used to initialize the prediction model in a receding horizon manner.

Further, the input is expressed in incremental form [11]:

$$x_{u_i}(t+1) = x_{u_i}(t) + \Delta u_i(t), \qquad \forall i \in \mathcal{N}_0, \qquad (4)$$

where $x_{u_i}(t) := u_{e_i}(t-1)$. This change of variables enables constraints on the rate of change of the control input, $\Delta u_i \in \Delta\mathcal{U}_i, i \in \mathcal{N}_0$, and ensures that the minimum cost is zero, when exactly tracking a constant reference in steady state.

Finally, the state vector is augmented with the reference signals, i.e., the setpoints for the performance outputs, here

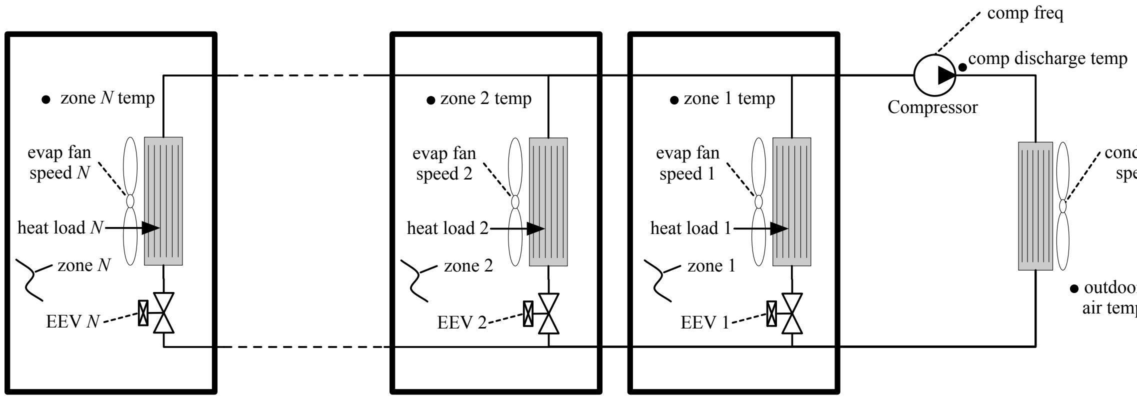

Fig. 1. Refrigerant piping arrangement of a multi-evaporator vapor compression system. The main actuators in the system are (i) the compressor frequency (CF), (ii) the outdoor (condenser) fan speed (ODF), and (iii) the electronic expansion valve (EEV). Note that in this work, an inner feedback loop computes the EEV from a setpoint representing the desired cooling capacity. This cooling capacity command (CCC) is determined by the MPC and viewed as a control input. The outputs of concern are the zone temperatures (Tri) and the compressor discharge temperature (Td).

the compressor discharge temperature and the zone temperatures. In particular, the reference zone temperature is assumed to be constant over the prediction horizon, i.e., $r_i(t+1) = r_i(t), i = 1, ..., N$, while the discharge temperature reference is defined as a linear function of the compressor frequency [12] that gives $r_0(t+1) = r_0(t) + \bar{B}_{r0}\Delta u_0(t)$. We also add integrators to the zone temperature tracking errors

$$\xi_i(t+1) = \xi_i(t) + T_s(r_i(t) - z_{e_i}(t)), \qquad \forall i = \mathcal{N}, \quad (5)$$

to achieve a more aggressive integral action besides that from the offsets in (3), hence obtaining faster convergence especially in the presence of model errors.

By augmenting the prediction model in this manner, the cost function is designed to minimize tracking error and integrated error between the measured and desired values of the performance outputs. Further considering the augmented model, define $w_0 := \text{col}(w_{e_0}, r_0)$, $x_0 := \text{col}(x_{e_0}, x_{u_0})$, $z_0 := r_0 - z_{e_0}$, $y_0 := y_{e_0}$ as the augmented exogenous signals, states, performance outputs and constrained outputs respectively, and the prediction model of the centralized subsystem can be written as:

$$\begin{aligned} w_0(t+1) &= w_0(t) + B_{r0}\Delta u_0(t) \quad (6)\\ x_0(t+1) &= A_{00}x_0(t) + \sum_{i=0}^{N} B_{0i}x_{u_i}(t) + \sum_{i=0}^{N} B_{0i}\Delta u_i(t)\\ z_0(t) &= E_0x_0(t) + H_0w_0(t), \quad y_0(t) = C_0x_0(t) + D_0w_0(t). \end{aligned}$$

Similarly, define variables $w_i := \text{col}(w_{e_i}, r_i)$, $x_i := \text{col}(x_{e_i}, x_{u_i}, \xi_i)$, $z_i := \text{col}(r_i - z_{e_i}, \xi_i), \forall i \in \mathcal{N}$, and the prediction model of the decentralized subsystems is written as:

$$\begin{aligned} w_i(t+1) &= w_i(t) \quad (7)\\ x_i(t+1) &= A_{ii}x_i(t) + A_{i0}x_0(t) + G_iw_i(t)\\ &\quad + \sum_{j=0}^{N} B_{ij}x_{u_j}(t) + \sum_{j=0}^{N} B_{ij}\Delta u_j(t)\\ z_i(t) &= E_ix_i(t) + H_iw_i(t), \qquad \forall\, i \in \mathcal{N}, \end{aligned}$$

where $w_i \in \mathbb{R}^{q_i}, x_i \in \mathbb{R}^{n_i}, u \in \mathbb{R}^{m_i}$ and $z_i \in \mathbb{R}^{p_i}, \forall i \in \mathcal{N}_0$. Although the actuator position $x_{u_i} \in \mathscr{X}_{u_i}$ is a subset of the augmented state $x_i \in \mathscr{X}_i$, $\forall i \in \mathcal{N}_0$, the state x_{u_i} has been pulled out in system model (6)-(7). As will be described later, this allows for monitoring the actuator separately under plug-and-play process, hence maintaining the overall system structure. Since $\mathscr{X}_{u_i} \subset \mathscr{X}_i$, there exists natural projections $\Omega_i : \mathscr{X}_i \to \mathscr{X}_{u_i}, \forall i \in \mathcal{N}_0$ from the augmented state x_i to the actuator position $x_{u_i} = \Omega_i x_i$.

Finally, the subsystem models are integrated by defining $w := \text{col}(w_0, ..., w_N)$, $x := \text{col}(x_0, ..., x_N)$ and $z = \text{col}(z_0, ..., z_N)$, resulting in the integrated model for the overall system:

$$\begin{aligned} w(t+1) &= w(t) + B_r\Delta u(t)\\ x(t+1) &= Ax(t) + B\Delta u(t) + Gw(t) \quad (8)\\ z(t) &= Ex(t) + Hw(t), \quad y_0(t) = Cx(t) + Dw(t), \end{aligned}$$

where $w \in \mathbb{R}^q, x \in \mathbb{R}^n, u \in \mathbb{R}^m, z \in \mathbb{R}^p$ are such that $q := \sum_{i=0}^{n} q_i, n := \sum_{i=0}^{n} n_i, m := \sum_{i=0}^{n} m_i, p := \sum_{i=0}^{n} p_i$. The nominal system matrices (A, B, E) have the following form:

$$A = \begin{bmatrix} A_{00} + B_{00}\Omega_0 & B_{01}\Omega_1 & \cdots & B_{0N}\Omega_N \\ A_{10} + B_{10}\Omega_0 & A_{11} + B_{11}\Omega_1 & \cdots & B_{1N}\Omega_N \\ \vdots & \vdots & \ddots & \vdots \\ A_{N0} + B_{N0}\Omega_0 & B_{N1}\Omega_1 & \cdots & A_{NN} + B_{NN}\Omega_N \end{bmatrix}$$

$$B = \begin{bmatrix} B_{00} & \cdots & B_{0N} \\ \vdots & \ddots & \vdots \\ B_{N0} & \cdots & B_{NN} \end{bmatrix}, \quad E = \begin{bmatrix} E_{00} & & \\ & \ddots & \\ & & E_{NN} \end{bmatrix}.$$

The integrated matrices (B_r, G, H, C, D) are also obtained, but they are not shown here due to the limited space. It is important to point out that the state matrix A seems not to preserve a lower block triangular form with the augmentation of actuator change rate. However, it is possible to express matrix A as $A := A_o + B\Omega$ with A_o being lower block triangular and $\Omega := \bigoplus_{i=0}^{N} \Omega_i$, and such structure will be exploited in the control synthesis.

III. Reconfigurable Model Predictive Control

Start/stop operation of the multi-evaporator VCS can be realized by a set of switched models to represent the changes of subsystem models, sensors and actuators, where the switched system framework provides useful tools for PnP analysis and control design. A switched model predictive control was first developed in this study, based on [13], [14]. Due to the space limit, the design of the switched MPC is not shown in the paper, whereas its simulation results will be used as a benchmark for assessing the performance of the reconfigurable MPC.

Although the model predictive control design based on switched systems allows one to achieve good performance with stability guarantees for start/stop operation of the multi-evaporator VCS through commissioning new prediction model and control design online, it requires calibration and design effort for each instance of a different number of active subsystems, and further requires storage of massive design parameters for execution, and thus a significant amount of memory for the microcontrollers.

For real-time implementation and production purposes, these challenges become significant impediments for control calibration and commissioning engineers. Therefore, starting from the analysis of model structural changes under plug-and-play process, this section proposes a reconfigurable model predictive control, which only requires a single master controller designed offline and provides a simple procedure for online reconfiguration. Further, this method retains stability guarantees for any realization of on/off subsystems, thus leading to considerably reduced design/calibration effort and memory load without compromising performance.

A. Plug-and-Play Model Representation

The PnP process for multi-evaporator VCS is characterized by changing the number of active zones in the decentralized subsystems (2). Hence, each zone is assigned with a switching signal $\varsigma_i(t) : \mathbb{Z} \to \{0, 1\}$, $\forall i \in \mathcal{N}$ where the binary switching signal $\varsigma_i(t)$ represents two operation modes for i-th indoor unit:

- ON: $\varsigma_i(t) = 1$,
- OFF: $\varsigma_i(t) = 0$.

Since the centralized subsystem is always on unless the entire machine is turned off, we assign $\varsigma_0(t) : \mathbb{Z} \to \{1\}$ for consistent notation. Denote $\varsigma(t) := \mathrm{col}(\varsigma_0(t), ..., \varsigma_N(t))$ the vector of switching signals such that $\varsigma(t) : \mathbb{Z} \to \mathcal{I} := \{1\} \times \{0, 1\} \times ... \times \{0, 1\}$. Let t_h denote the time when the h-th switch occurs and define $\mathcal{T}_h := \{t_h : h \in \mathbb{Z}\}$ as the set of switching time instants. It is assumed that $\varsigma(t)$ is constant over the interval $[t_h, t_{h+1})$, namely $\varsigma(t + 1) = \varsigma(t), t \in [t_h, t_{h+1})$. As a result, the centralized PnP prediction model can be written as:

$$w_0(t+1) = w_0(t) + B_{r0}\Delta u_0(t) \tag{9}$$
$$x_0(t+1) = A_{00}x_0(t) + \sum_{i=0}^{N} \varsigma_i(t)B_{0i}x_{u_i}(t) + \sum_{i=0}^{N} \varsigma_i(t)B_{0i}\Delta u_i(t)$$
$$z_0(t) = E_0x_0(t) + H_0w_0(t), \quad y_0(t) = C_0x_0(t) + D_0w_0(t).$$

Similarly, the decentralized subsystem can be written as:

$$\begin{aligned} w_i(t+1) &= w_i(t) + B_{r0}\Delta u_0(t) \\ x_i(t+1) &= A_{ii}x_i(t) + \varsigma_i(t)A_{i0}x_0(t) + \varsigma_i(t)G_iw_i(t) \\ &\quad + \varsigma_i(t)\sum_{j=0}^{N}\varsigma_j(t)B_{ij}x_{u_j}(t) + \varsigma_i(t)\sum_{j=0}^{N}\varsigma_j(t)B_{ij}\Delta u_j(t) \\ z_i(t) &= E_ix_i(t) + H_iw_i(t), \qquad \forall\, i \in \mathcal{N}. \end{aligned} \tag{10}$$

The representation in (9)-(10) is motivated by the fact that once the i-th evaporator is turned off, the corresponding i-th actuator x_{u_i}, Δu_i, and exogenous signal w_i no longer affect the dynamics. Moreover, the coupling term A_{i0} is also cancelled, implying that the associated zone temperature is no longer affected by the states of centralized refrigerant system, and therefore the zone temperature evolves according to its (unforced) natural thermal dynamics.

B. Model Predictive Control Design

Model predictive control for tracking typically consists of a steady state characterization and receding horizon optimization [15]. The steady state characterization determines, for a given constant signal w_s, a set of steady state solutions of state and input $(x_s, \Delta u_s)$ corresponding to the desired output z_s, satisfying the system equation (8):

$$\begin{aligned} w_s &= w_s + B_r\Delta u_s \\ x_s &= Ax_s + B\Delta u_s + Gw_s \\ z_s &= Ex_s + Hw_s. \end{aligned} \tag{11}$$

Instead of finding the pairs $(x_s, \Delta u_s)$ corresponding to each w_s [10] by solving (11), we are interested in finding parameterized solutions $x_s = \Pi w_s, \Delta u_s = \Gamma w_s$ for $w_s \in \mathcal{W}_s$, where $\Pi \in \mathbb{R}^{n\times q}, \Gamma \in \mathbb{R}^{m\times q}$ and $\mathcal{W}_s$ is a compact set in $\mathbb{R}^q$. Recalling that the performance output (tracking error and integrated error) aims at $z_s = 0$ and control input rate aims at $\Delta u_s = 0$ in steady state, the equation (11) can thus be rewritten as:

$$\begin{bmatrix} I - A & -B \\ -E & 0 \end{bmatrix} \begin{bmatrix} \Pi \\ 0 \end{bmatrix} = \begin{bmatrix} G \\ H \end{bmatrix}. \tag{12}$$

Solutions to (11) and (12) exist if the set of invariant zeros of the triplet (E, A, B) is disjoint from the unitary spectrum of the exosystem model. In particular, when the system is over-actuated $m > p$ (as in this case), there exists multiple solutions and the explicit solution can be derived from geometric characterization [16].

The reconfigurability of model predictive control is achieved by employing a decentralized (block diagonal) terminal cost for each subsystem, where each sub-block can be easily included or removed from the cost functions through simple matrix operation without need to redesign the remainder of the terminal cost. As it will be justified in the following, such an approach does not require to rebuild the (switched) prediction model, allowing one to reduce to the minimum online adjustment of the receding horizon optimization problem and ultimately of the quadratic programming problem.

For notational convenience, the MPC controller is formulated by separating each subsystem. The MPC solves a receding horizon optimization problem at each sampling time t, given the switching signal $\varsigma(t)$, of the form

$$\min_{U,\epsilon} \quad \sum_{k=0}^{N_m-1} \sum_{i=0}^{N} \varsigma_i(t) \|z_{i,k|t}\|_{Q_i}^2 + \varsigma_i^{-1}(t)\|\Delta u_{i,k|t}\|_{R_i}^2 + \sum_{i=0}^{N} \varsigma_i(t)\|x_{i,N_m|t} - \Pi_i w_{N_m|t}\|_{P_i}^2 + \|\epsilon\|_T^2 \tag{13a}$$

$$\begin{aligned} & w_{0,k+1|t} = w_{0,k|t} + B_r \Delta u_{0,k|t}, \quad w_{0,0|t} = w_0(t) \\ & x_{0,k+1|t} = A_{00} x_{0,k|t} + \sum_{i=0}^{N} B_{0i} x_{u_i,k|t} + \sum_{i=0}^{N} B_{0i} \Delta u_{i,k|t} \\ & z_{0,k|t} = E_0 x_{0,k|t} + H_0 w_{0,k|t}, \\ & y_{0,k|t} = C_0 x_{0,k|t} + D_0 w_{0,k|t}, \\ & y_{0,k|t} \in \mathcal{Y}_\epsilon, \quad x_{u_{0,k|t}} \in \mathcal{U}_0, \quad \Delta u_{0,k|t} \in \Delta\mathcal{U}_0 \end{aligned} \tag{13b}$$

$$\begin{aligned} & w_{i,k+1|t} = w_{i,k|t} \\ & x_{i,k+1|t} = A_{ii} x_{i,k|t} + A_{i0} x_{0,k|t} + G_i w_{i,k|t} \\ & \qquad + \sum_{j=0}^{N} B_{ij} x_{u_j,k|t} + \sum_{j=0}^{N} B_{ij} \Delta u_{j,k|t} \\ & z_{i,k|t} = E_i x_{i,k|t} + H_i w_{i,k|t} \\ & x_{u_{i,k|t}} \in \mathcal{U}_i, \quad \Delta u_{i,k|t} \in \Delta\mathcal{U}_i, \qquad \forall\, i \in \mathcal{N}, \end{aligned} \tag{13c}$$

where $Q_i \in \mathbb{R}^{p_i \times p_i}, R_i \in \mathbb{R}^{m_i \times m_i}, P_i \in \mathbb{R}^{n_i \times n_i}$, $i \in \mathcal{N}_0$ represent stage cost on output, input and terminal cost of i-th subsystem respectively, and $\Pi_i \in \mathbb{R}^{n_i \times q}$ is the steady state matrix of i-th subsystem such that $x_{s,i} = \Pi_i w_s$ and $\Pi := \mathrm{col}(\Pi_0, ..., \Pi_n)$. N_m is the prediction horizon and the optimization vector is $U := \mathrm{col}(\Delta u_{0,0|t}, ..., \Delta u_{N,0|t}, ..., \Delta u_{0,N_m-1|t}, ..., \Delta u_{N,N_m-1|t})$.

Notice that only the cost function (13a) is modified online under the PnP process according to the switching signal $\varsigma(t)$, while the prediction models (13b)-(13c) and constraints are kept unchanged. Considering the interconnected nature of the overall system, it is critical to decouple the inactive subsystem from decision making in the receding horizon optimization. Without loss of generality, it is assumed that i-th subsystem is turned off in the forthcoming analysis. Then, the decoupling objective can be achieved, leveraging on the system structure, with the following rules:

1) For i-th actuator that is shut off, it follows $x_{u_i,k|t} \equiv 0$, $\forall k = 0, ..., N_m$, $\Delta u_{i,k|t} \equiv 0$, $\forall k = 0, ..., N_m - 1$, which guarantees that the decoupled i-th actuator will have no influence on any j-th subsystem $j \in \mathcal{N}_0$. Moreover, $w_{i,k|t} \equiv 0$, $\forall k = 0, ..., N_m$ such that the exogenous signal $w_{i,k|t}$ does not affect the state $x_{i,k|t}$ and the steady state solution $\Pi_j w_{N_m|t}, \forall j \in \mathcal{N}_0$. This can be achieved by initializing $x_{u_i}(t) = 0$, $w_i(t) = 0$ and imposing infinite penalty[1] $\varsigma_i^{-1}(t) R_i$ on $\Delta u_{i,k|t}$ in the cost function of receding horizon optimization (13a).
2) The constraints on $x_{u_{i,k|t}}$, $\forall k = 0, ..., N_m$ and $\Delta u_{i_{k|t}}$, $\forall k = 0, ..., N_m - 1$ are always inactive in the optimization. This is ensured by the assumption that $\mathcal{U}$, $\Delta\mathcal{U}$ include the origin in their interiors.
3) The predicted state $x_{i,k|t}$ and output $z_{i,k|t}$ trajectories for i-th subsystem are not observable in the cost function, $\forall t = 0, ..., N_m$, which can be achieved by zeroing out the penalty as $\varsigma_i(t) P_i$ and $\varsigma_i(t) Q_i$ on i-th subsystem.
4) The predicted state trajectory $x_{i,k|t}, i \in \mathcal{N}$ has no influence on the other state $x_{j,k|t}$ trajectory, $\forall t = 0, ..., N_m, \forall j \in \mathcal{N}_0, j \neq i$. This is guaranteed by the interconnected structure (1)-(2), where the state of i-th subsystem is not directly connected to that of any other subsystems.
5) Given any $\varsigma_i(t), i \in \mathcal{N}_0$ and the corresponding block diagonal stage cost and terminal cost matrices

$$\mathcal{Q}_\varsigma := \bigoplus_{i=0}^{N} \varsigma_i(t) Q_i, \; \mathcal{R}_\varsigma := \bigoplus_{i=0}^{N} \varsigma_i^{-1}(t) R_i, \; \mathcal{P}_\varsigma := \bigoplus_{i=0}^{N} \varsigma_i(t) P_i, \tag{14}$$

where $\mathcal{Q}_\varsigma \in \mathbb{R}^{p \times p}, \mathcal{R}_\varsigma \in \mathbb{R}^{m \times m}, \mathcal{P}_\varsigma \in \mathbb{R}^{n \times n}$, there exists a terminal control $\Delta u := \mathcal{K}_\varsigma(x - \Pi w)$ that satisfies the stabilizing condition for the MPC controller:

$$\begin{aligned} & (A_\varsigma + B_\varsigma \mathcal{K}_\varsigma)^T \mathcal{P}_\varsigma (A_\varsigma + B_\varsigma \mathcal{K}_\varsigma) - \mathcal{P}_\varsigma \\ & \qquad \preceq -E^T \mathcal{Q}_\varsigma E - \mathcal{K}_\varsigma^T \mathcal{R}_\varsigma \mathcal{K}_\varsigma, \end{aligned} \tag{15}$$

where A_ς, B_ς are the system matrices corresponding to the switching signal $\varsigma(t)$. Such terminal control synthesis will be explored in the following section.

Following the above principles, the actuator and predicted state trajectory for i-th subsystem that is turned off is successfully decoupled from the online optimization without need to rebuild the prediction model (as in the switched models). Moreover, the cost function in the optimization can be easily reconfigured online, without need to redesign terminal cost $P_j, j \in \mathcal{N}_0, j \neq i$ for any other subsystems under PnP process.

C. Terminal Cost and Control Design

As discussed in the previous section, the objective is to design a block diagonal terminal cost P_ς (14) with a structured terminal control K_ς that satisfies the stabilizing condition (15) for any combination of active subsystems. The following proposition shows that a properly structured terminal cost matrix and terminal controller can be used to guarantee stability when zones are deactivated.

Proposition 3.1: Consider a terminal linear controller of the form

$$\begin{aligned} & \Delta u_0 = \varsigma_0(t) K_{00}(x_0 - \Pi_0 w) + \sum_{i=1}^{N} \varsigma_i(t) K_{0i}(x_i - \Pi_i w) \\ & \Delta u_i = \varsigma_i(t) K_{ii}(x_i - \Pi_i w), \qquad \forall i = 1, ..., N, \end{aligned} \tag{16}$$

[1]When solving the quadratic optimization, the infinity penalty is replaced by an arbitrarily large value related to the problem condition number.

where the integrated control gain matrix $\mathcal{K}_\varsigma$ is expressed as

$$\mathcal{K}_\varsigma = \begin{bmatrix} \varsigma_0(t)K_{00} & \varsigma_1(t)K_{01} & \cdots & \varsigma_N(t)K_{0N} \\ 0 & \varsigma_1(t)K_{11} & \cdots & 0 \\ \vdots & \vdots & \ddots & \vdots \\ 0 & 0 & \cdots & \varsigma_N(t)K_{NN}, \end{bmatrix} \quad (17)$$

and a block diagonal terminal cost P_ς of the form (14). The stability condition (15) is satisfied for any switching signal $\varsigma(t)$ if the sub-matrices $\{P_i, i \in \mathcal{N}_0\}$ and $\{K_{0i}, K_{ii}, i \in \mathcal{N}_0\}$ satisfy

$$(A + B\mathcal{K})^T \mathcal{P}(A + B\mathcal{K}) - \mathcal{P} \preceq -E^T \mathcal{Q} E - \mathcal{K}^T \mathcal{R} \mathcal{K}, \quad (18)$$

for the master problem when all the decentralized subsystems are active $(\mathcal{P}, \mathcal{K}, \mathcal{Q}, \mathcal{R}) := \{(\mathcal{P}_\varsigma, \mathcal{K}_\varsigma, \mathcal{Q}_\varsigma, \mathcal{R}_\varsigma) : \varsigma_i(t) = 1, \forall i \in \mathcal{N}_0\}$.

Proof: The proof is omitted for space limitation. ■

Remark 2: Considering the structure of the proposed terminal control (16), it is interesting to find that the centralized control input Δu_0 feeds back the state information from all subsystems. Conversely, since the decentralized states are not directly connected to any other subsystems in the open loop system, the control input $\Delta u_i, \forall i \in \mathcal{N}$ only feeds back its own state information.

IV. Simulation Results

In this section, the proposed reconfigurable model predictive controller is designed according to the procedures outlined in Section III, which consists of a master controller designed and tuned for two evaporators turned on, and a procedure to automatically reconfiguring when a single evaporator is on. Additionally, a switched model predictive controller consisting of two MPC controllers, one for a single evaporator turned on and another for two evaporators turned on, is designed. At switching events when an evaporator state changes, the corresponding controller is deployed. The performance of both controllers is compared in a simulation of a two-zone multi-evaporator vapor compression system, where one zone is periodically switched on and off.

The plant model used in the following simulations and the corresponding prediction models used in the MPC designs are derived from experimental data collected on a two-zone home air conditioner in controlled laboratory conditions. With fixed heat loads applied in adiabatic test chambers and the system operating at steady state, step inputs are applied to the actuators of the open loop system (compressor frequency, cooling capacity commands, and outdoor fan speeds) and measurements of the system outputs are collected, enabling the creation of a state space model of the plant in the form of equations (1)-(2).

In the following simulations, the sampling time of the estimator is 1 sec, and the control inputs are updated every 60 sec. The prediction horizon has a length of 32 minutes, while the predicted control inputs were optimized over the first 16 minutes, and the terminal controller is used over the remaining 16 minutes. A 240 minute simulation is conducted, where the evaporator in zone A is on and the reference temperature is held constant at 25^oC, while the evaporator in zone B is switched between the on and off state every 60 min with the reference temperature set at 18^oC when it is turned on.

The simulation results are shown in Fig. 2, in which Fig. 2A shows the actuator positions and Fig. 2B shows the performance and constrained outputs. The performance of the proposed reconfigurable MPC method, for which reduced zone controllers are synthesized from a master controller, is compared to the traditional switched MPC method, where each controller is designed offline and stored in memory. The closed loop performance is shown to be largely similar, however, the number of system matrices stored in memory and the design/tuning parameters required for the reconfigurable method are substantially fewer, as illustrated in Table II.

Comparing the performances of reconfigurable MPC to those of switched MPC, negligible difference can be observed in the overall simulation results, except in slightly smaller decreasing rates of outdoor fan (ODF) speed when the evaporator in zone B is shut off. This may be caused by the slightly more conservative terminal cost as computed in reconfigurable MPC method by the required block diagonal structure of $\mathcal{P}_\varsigma$ in equation (14).

In summary, the simulation confirms that the proposed approach effectively decoupled the trajectory with respect to zone B when it was turned off from decision making in the receding horizon optimization through simple online adjustment of cost function without rebuilding the prediction model and compromising the regulation performance.

Finally, to understand the relationship between the number of evaporators and the tuning effort and memory storage requirement to build and solve the quadratic programming problem, Table II shows a comparison of the size of the system matrices to build the prediction model and of the design parameters to build the cost function. It is apparent that the switched MPC method yields exponential growth in the sizes of the system matrices and design parameters (*e.g.* tuning weights) as the number of evaporators increases, and ultimately results in unrealistically large numbers for 50 evaporators (which is a typical number for commercial multi-evaporator air conditioners).

V. Conclusions and Future Work

In this paper, model predictive control has been investigated to control multi-evaporator vapor compression ma-

TABLE II

Comparison of System Matrices (SM), Design Parameters (DP), Approximated Storage Load (SL) between Different MPC Approaches. The Reconfigurable MPC method requires many fewer parameters to design, tune and validate.

NO. of Zones	Real Numbers in (SM) and (DP) and Megabytes of (SL) to Build QP Online					
	Switched MPC			Reconfigurable MPC		
	(SM)	(DP)	(SL) MB	(SM)	(DP)	(SL) MB
2	3.5e3	2.5e3	0.092	880	613	0.023
8	1.25e6	9.25e5	33.3	4.9e3	3.6e3	0.13
50	1.4e20	1.1e20	3.8e15	1.24e5	9.5e4	3.4

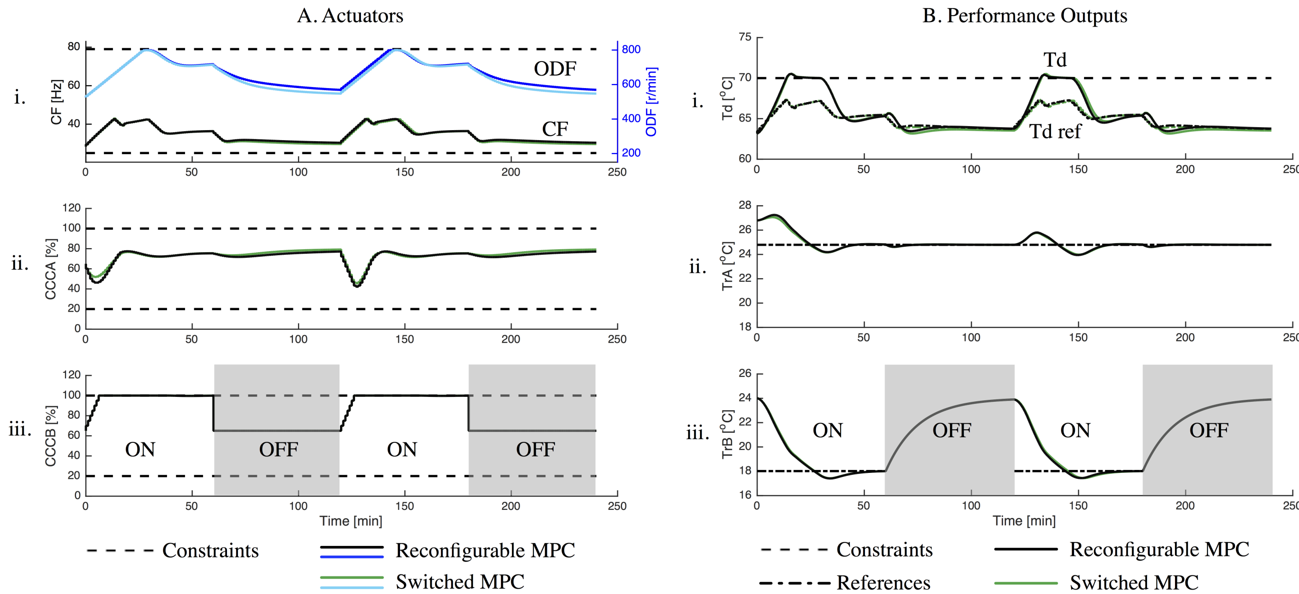

Fig. 2. Simulation of a two-zone multi-evaporator VCS where zone B is periodically switched off. Performance of the proposed reconfigurable MPC method is compared to the traditional switched MPC method (where each controller is. The closed loop performance is shown to be largely similar, however, the number of system matrices stored in memory and the design/tuning parameters required for the reconfigurable method are substantially fewer.

chine, particularly focusing on turning evaporators on and off. As opposed to a switched model predictive control, which requires the prediction model and the control system to be reconstructed when any subsystem is turned on or off and thus is expensive in terms of engineering calibration and deployment of control parameters, a reconfigurable model predictive control is proposed leveraging the system model structure, leading to online adjustment of the control structure with stability guarantees. Principles to effectively decouple the inactive subsystems from decision making (without rebuilding the prediction model) from the optimization are discussed, and stability conditions are proved. Simulation studies confirmed that the proposed approach retained the same tracking performance of zone temperatures while significantly reducing the control design parameters and design effort compared to the switched control design approach. Future work will focus on the experimental validation of the proposed approach.

References

[1] N. Jain, D. J. Burns, S. Di Cairano, C. R. Laughman, and S. A. Bortoff, "Model predictive control of vapor compression systems," in *15th International Refrigeration and Air Conditioning Conference at Purdue, July, 2014*, 2014.

[2] M. Wallace, B. Das, P. Mhaskar, J. House, and T. Salsbury, "Offset-free model predictive control of a vapor compression cycle," *Journal of Process Control*, vol. 22, no. 7, pp. 1374–1386, 2012.

[3] J. Koeln and A. Alleyne, "Scalable model predictive control for multi-evaporator vapor compression systems," in *American Control Conference (ACC), 2014*, June 2014, pp. 392–397.

[4] M. S. Elliott and B. P. Rasmussen, "Decentralized model predictive control of a multi-evaporator air conditioning system," *Control Engineering Practice*, vol. 21, no. 12, SI, pp. 1665–1677, DEC 2013.

[5] J. P. Koeln and A. G. Alleyne, "Decentralized Controller Analysis and Design for Multi-Evaporator Vapor Compression Systems," in *American Control Conference (ACC), 2013*, 2013, pp. 437–442.

[6] J. Stoustrup, "Plug & play control: Control technology towards new challenges," *European Journal of Control*, vol. 15, no. 3, pp. 311–330, 2009.

[7] J. Bendtsen, K. Trangbaek, and J. Stoustrup, "Plug-and-play control: Modifying control systems online," *IEEE Transactions on Control Systems Technology*, vol. 21, no. 1, pp. 79–93, 2013.

[8] S. Riverso, M. Farina, and G. Ferrari-Trecate, "Plug-and-play model predictive control based on robust control invariant sets," *Automatica*, vol. 50, no. 8, pp. 2179–2186, 2014.

[9] M. N. Zeilinger, Y. Pu, S. Riverso, G. Ferrari-Trecate, and C. N. Jones, "Plug and play distributed model predictive control based on distributed invariance and optimization," in *52nd Annual Conference on Decision and Control (CDC)*. IEEE, 2013, pp. 5770–5776.

[10] G. Pannocchia and J. B. Rawlings, "Disturbance models for offset-free model-predictive control," *AIChE journal*, vol. 49, no. 2, pp. 426–437, 2003.

[11] S. Di Cairano, H. E. Tseng, D. Bernardini, and A. Bemporad, "Vehicle yaw stability control by coordinated active front steering and differential braking in the tire sideslip angles domain," *IEEE Transactions on Control Systems Technology*, vol. 21, no. 4, pp. 1236–1248, 2013.

[12] D. Burns and C. Laughman, "Extremum seeking control for energy optimization of vapor compression systems," in *14th International Refrigeration and Air Conditioning Conference at Purdue, July, 2012*.

[13] S. Di Cairano, "Model adjustable predictive control with stability guarantees," in *American Control Conference (ACC), 2015*, July 2015, pp. 226–231.

[14] M. Lazar, "Model predictive control of hybrid systems: Stability and robustness," 2006.

[15] D. Limón, I. Alvarado, T. Alamo, and E. F. Camacho, "MPC for tracking piecewise constant references for constrained linear systems," *Automatica*, vol. 44, no. 9, pp. 2382–2387, 2008.

[16] J. Zhou, M. Canova, and A. Serrani, "Stability and feasibility of predictive inverse model allocation for constrained over-actuated linear systems," in *American Control Conference (ACC), 2015*, July 2015, pp. 4567–4572.